JOURNAL OF MATERIALS SCIENCE **34** (1999) 3189–3202

Influence of the preparation conditions on the synthesis of high surface area SiC for use as a heterogeneous catalyst support

N. KELLER, C. PHAM-HUU, S. ROY, M. J. LEDOUX
Laboratoire de Chimie des Matériaux Catalytiques, ECPM, 25, rue Becquerel BP08, 67087 Strasbourg Cedex 2, France
E-mail: ledoux@cournot.u-strasbg.fr

C. ESTOURNES, J. GUILLE
Groupe des Matériaux Inorganiques, IPCMS, ECPM-ULP-CNRS, UMR 7504, 23, rue du Loess, 67037 Strasbourg Cedex, France

The influence of different parameters (temperature, duration and SiO source) on the synthesis of silicon carbide SiC according to the gas-solid reaction between SiO vapors and activated charcoal was investigated. The material obtained retained the general shape of the activated charcoal, which is an advantage because of the difficulty in post shaping SiC, due to the high strength of the material. High temperature (>1250 °C) and long reaction duration led to a high $C^* \rightarrow SiC$ conversion but with a relatively low surface area (20–25 $m^2 \cdot g^{-1}$) due to sintering via the surface diffusion phenomenon. The combination of a lower reaction temperature (1200 °C), longer reaction duration (15 h) and high $(Si + SiO_2)/C^*$ weight ratio allowed SiC to be obtained with a surface area of around 50 $m^2 \cdot g^{-1}$, which can be used as a support material for heterogeneous catalysis.

1. Introduction

In general, commercial catalysts are biphasic being composed of a support material and one or more active phase components (metal or oxide). Support materials provide a porous framework permitting access to the active phase for the reactants and free exit for the products from the catalyst particles. The support must be able to disperse the active phase in order to increase the active surface in contact with the reactant. It must also have high mechanical and thermal stability in order to avoid surface area collapse during reaction or oxidative regeneration which can induce the formation of hot spots. All of this must be achieved with the support being chemically resistant, cheap, abundant and not strategically limited. Easy preparation of large, well characterized samples of the support material is also necessary.

Usually, industrial supports are based on high surface area γ-Al_2O_3, pure or doped with different elements in order to improve the mechanical and thermal stability of the support [1, 2]. Under normal reaction conditions, γ-Al_2O_3 is stable, but at temperatures between 700 and 1000 °C and in the presence of steam, a phase transformation occurs, first to metastable δ- and θ-Al_2O_3 leading to the formation of α-Al_2O_3 with a low surface area [3]. In addition, the chemical interaction between the alumina support and the active phase leads to the formation of a new compound, resulting in loss of the active phase and as a consequence, the catalytic activity [4]. The strong chemical interaction of the alumina support with the active phase also hinders recovery of the latter at the end of the catalyst life-time.

Silicon carbide (SiC) ceramic materials have been developed for use in a broad range of applications, including biomedical materials, high temperature semiconducting devices, synchrotron optical elements, and lightweight/high strength structures [5]. SiC exhibits a high thermal conductivity, high resistance towards oxidation (due to the formation of SiO_2 layers), high mechanical strength and chemical inertness, properties required for heterogeneous catalyst support materials. This latter property is particularly useful during oxidative regeneration (frequently used in the heterogeneous catalysis field in order to burn off the carbonaceous deposit on the catalyst surface during the reaction) and, in general, high thermal conductivity allows new options in designing processes which are highly exothermic or endothermic. In certain conditions the formation of SiO_2 by oxidation can be a serious drawback to the use of SiC as a catalyst support. Finally, the chemical inertness of the support allows easy recovery of the active phase without severe processes such as those generally employed for alumina-based spent catalysts.

All of these advantages lead to the conclusion that silicon carbide is a promising candidate for a heterogeneous catalyst support. However, for SiC to be useful as a catalyst support it must be prepared in a high

surface area form ($\geq$20–30 $m^2 \cdot g^{-1}$) and an inability to do so has been the limiting factor in its application in catalysis. For this reason, considerable attention has been focused on developing preparative methods that will yield high surface area materials from different reaction types such as solid-solid, gas-solid and gas-phase reactions [6–11]. More detailed reviews concerning new synthetic routes to high surface area non-oxide materials have recently been reported by Chorley and Lednor [12] and by Carty and Lednor [13].

It has been reported by Ledoux and co-workers [6–9] that high surface area (>20–40 $m^2 \cdot g^{-1}$) SiC can be prepared at relatively low temperature by the gas-solid reaction between activated charcoal and SiO vapor. The as-prepared material can be used, as efficiently as the traditional alumina support, for several reactions such as hydrodesulfurization [7], automotive exhaust-pipe reactions [14], isomerization reactions [15] and in the selective oxidation of H_2S into elemental sulphur [16]. Concerning the last cases, the chemical inertness of the support avoids the loss of catalytic activity by formation of side products such as aluminate (automotive exhaust pipe reaction) and aluminium sulfate (desulfurization process).

The aim of the present article is to report a more detailed study of the influence of the preparation parameters on the synthesis of high surface area SiC, and the optimization of the SiC conversion and the surface area by a combination of all the parameters studied. The characteristics of the prepared material were followed by several characterization techniques. A more detailed characterization will be devoted to the influence of preparation parameters on the evolution of the ceramic surface area, conversion, porosimetry and also the mechanism of the SiO vapor generation.

2. Experimental

2.1. SiC synthesis

The silicon carbide was prepared by the gas-solid reaction between high surface area activated charcoal and SiO vapor under dynamic vacuum. The SiO vapor was generated by heating a mixture of Si and SiO_2 in the temperature range 1200–1400 °C according to the following equation

$$Si + SiO_2 \leftrightarrow 2SiO \quad (1)$$

The generated SiO vapour was then led toward the upper stage of the reactor where the reactant carbon was located, as shown in Fig. 1a and b. The reaction between SiO and C occured at a lower temperature (1200–1350 °C) according to the reaction

$$SiO + 2C \rightarrow SiC + CO \quad (2)$$

and allowed the production of high surface area SiC. The schematic diagram of the apparatus used is presented in Fig. 1a. The activated charcoal and the Si/SiO_2 mixture were located in a densified alumina crucible (inner diameter 60 mm, length 100 mm) which was not active towards the reactants or material formed (Fig. 1b). The alumina crucible was introduced into an impermeable densified silicon carbide tube (inner diameter 130 mm, length 800 mm). This configuration allowed a relatively low residual pressure (0.05 Torr). The reactor was heated by four lanthanum chromite heater elements and controlled by two temperature regulators Eurotherm 818P. The vacuum was obtained using a turbo pump. After reaction, the final silicon carbide was cooled under dynamic vacuum to room temperature.

Before starting the reaction, the activated charcoal was outgassed at 1000 °C under dynamic vacuum for 2 h in order to desorb the impurities from its surface. The CO formed from the reaction between SiO and C was rapidly pumped out of the reaction zone, pulling the equilibrium towards SiC formation. The yield of the reaction was strongly limited by the formation of CO.

The samples obtained were divided into two parts: the first for characterization without further treatment (after synthesis) and the second after a calcination in air at 600 °C for 2 h. The latter operation was performed in order to burn off the remaining activated charcoal located in the core of the ceramic.

2.2. Characterization techniques

The silicon carbide was characterized by several techniques such as powder X-ray diffraction (XRD), surface area measurements using the BET method, scanning electron microscopy (SEM), high-resolution electron microscopy (HRTEM), thermogravimetric analysis (TGA), and differential thermal analysis (DTA).

X-ray powder diffraction (XRD) was used for structural characterization of the samples. XRD measurements were performed on a Siemens Model D-5000 diffractometer with CuK_α monochromatic radiation ($\lambda = 1.5406$ Å). The sample was crushed in an agate mortar and the powder was packed into 0.5 mm depressions of 40 × 44 mm polymer slides. Samples were exposed to radiation from 10 to 100° of 2θ angle with a step scan mode (step = 0.02° 2θ with a step to step time of 10 s). The nature of the crystalline phases present in the sample was checked using the data base of the Joint Committe on Powder Diffraction Standards (JCPDS).

Thermogravimetry (TG) and differential thermal analysis (DTA) were performed using a Balzer thermoanalyzer. Typical sample size used for analysis was 0.250–0.425 mm with a heating rate of 5 °C min^{-1}. This technique allowed the exact determination of the temperature at which all the remaining charcoal was burned.

The specific surface area (S_g) was obtained from nitrogen physisorption at −196 °C using a Coulter AS 3100 sorptometer. The standard pretreatment consisted of heating the sample under dynamic vacuum at 150 °C for 1 h in order to remove the adsorbed water and other impurities. The measurement was made at liquid-nitrogen temperature, with nitrogen (Air Liquide, 99.95%) as the adsorbate gas. The porosimeter allowed the measurement of different kinds of surface area contribution: S_{BET} is the surface area of the sample calculated from the nitrogen isotherm using the BET Method, S_{BJH} is the surface area of all the pores except micropores calculated from the N_2 desorption isotherm,

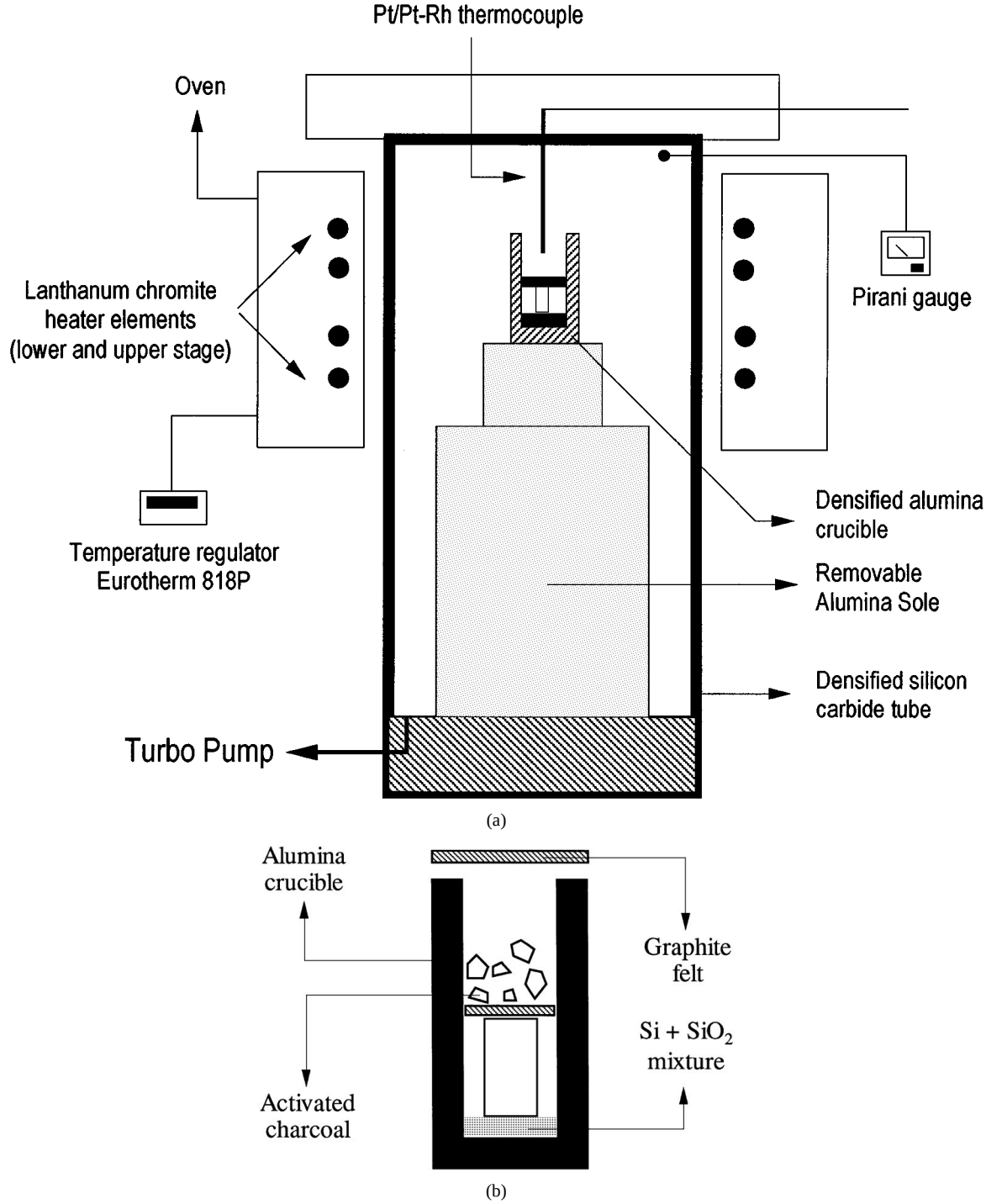

Figure 1 (a) Schematic diagram of the apparatus used in the high surface area SiC synthesis and (b) schematic diagram of the crucible used in the high surface area SiC synthesis.

$S_{micropore}$ is the surface area of the micropores calculated using the *t*-plot method developed by De Boer and co-workers [17].

The morphology of the silicon carbide was observed by SEM using a Jeol Model JSM-850 operated at 20 kV and 10 mA. The samples were covered with gold in order to avoid the charge effect during analysis. The low magnification of the examined samples allowed better access to the general shape of the final material compared to that of the starting activated charcoal.

High Resolution Transmission Electron Microscopy (HRTEM) was used to characterize the microstructure of the material. The TEM experiments were carried out with a Topcon EM-002 B microscope working at 200 kV equipped with a Kevex analytical system allowing the detection of light elements. The high-resolution objective lens with a spherical aberration coefficient (C_s) of 0.5 mm, allowed a point-to-point resolution of this equipment of 1.8 Å. Samples were supported on holey carbon-coated copper grids by simply grinding the specimen between glass plates and bringing the powder into contact with the grid. To prevent artifacts due to contamination, no solvents were used at any stage of the sample preparation. Great care was taken during HRTEM observations in order to avoid heating effects from the electron beam.

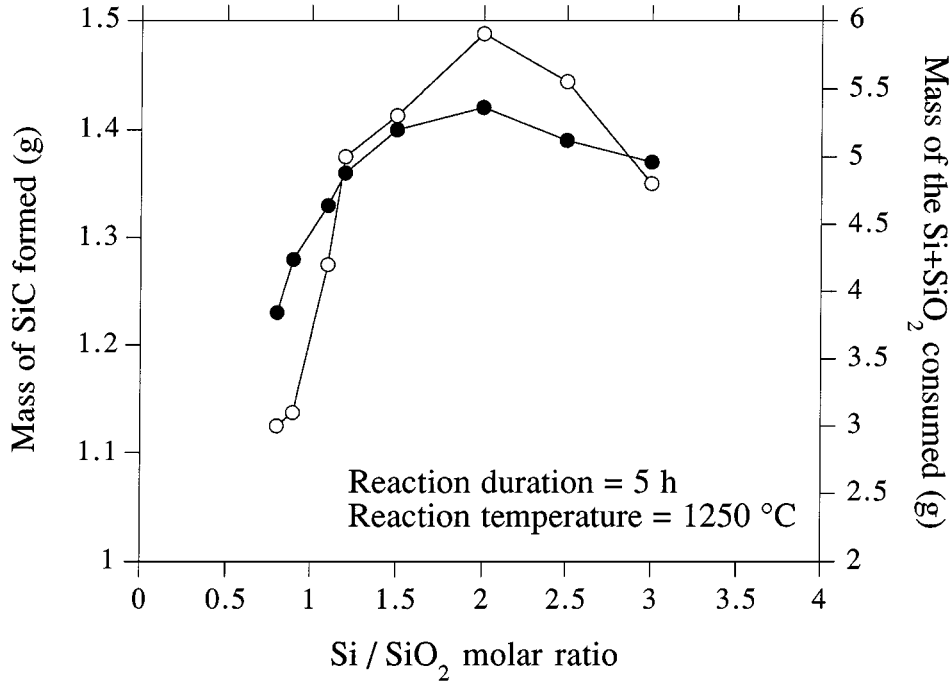

Figure 2 Influence of the Si/SiO_2 ratio on the amount of SiC formed (○) and source mixture consumed (●).

3. Results

3.1. Evolution of the support characteristics as a function of the reaction parameters

3.1.1. Influence of the molar ratio of Si/SiO_2 on the $C \rightarrow SiC$ conversion

It has been reported in previous work [18] that the molar ratio of the Si/SiO_2 source could play an important role in the formation of SiC, probably by modifying the partial pressure of SiO vapour as will be discussed later. The saturation of the active sites, present on the activated charcoal, by SiO molecules at the beginning of the synthesis probably improved the nucleation sites for SiC formation and thus increased the final yield of SiC, as already observed by Peschiera [18]. In this section, the influence of the molar ratio of the Si/SiO_2 mixture on the final conversion of SiC will be investigated.

A series of experiments were conducted with different molar ratios of Si/SiO_2 mixture at 1250 °C for 5 h and the results obtained are presented in Fig. 2. Increasing the Si/SiO_2 molar ratio led to a volcano curve as far as the final conversion of the activated charcoal was concerned. The amount of SiC reached a maximum when the molar ratio Si/SiO_2 was 2. For higher Si/SiO_2 molar ratios the quantity of SiC produced slowly decreased. The maximum corresponded to a yield of 59% in terms of carbon transformed into SiC.

3.1.2. Influence of the reaction temperature, the duration and the $(Si + SiO_2)/C^*$ ratio on the support surface area and porosity

The influence of the reaction temperature with a reaction duration of 5 h on the pore size distribution of the calcinated SiC is presented in Fig. 3. The pore size distribution of the SiC material synthesized at a temperature ≤1250 °C was bimodal with the average pore sizes centered around 5 and 20 nm. At higher temperatures, the small pores (4–5 nm) collapsed and only a pore distribution centered around 20 nm was observed along with the decrease in the material surface area (Table I). Decreasing the reaction temperature to less than 1200 °C did not allow the transformation of the activated charcoal to SiC with a significant conversion.

TABLE I Characteristics of SiC as a function of the reaction temperature. Reaction conditions: Si/SiO_2 molar ratio = 2, reaction duration = 5 h, $(Si + SiO_2)/C^*$ weight ratio = 2.5. The BET surfaces areas reported were those obtained after calcination of the SiC material after synthesis, in air at 600 °C for 2 h

Reaction temperature (°C)	BET surface area ($m^2 \cdot g^{-1}$)	$C^* \rightarrow$ SiC conversion (%)
1200	105	21
1250	46	59
1300	26	77

The influence of the reaction duration was investigated at reaction temperatures of 1250 and 1300 °C with a (Si/SiO_2) molar ratio of 2. The results are summarized in Table II. High surface area SiC was formed rapidly

TABLE II Characteristics of SiC as a function of the reaction duration and temperature. Reaction conditions: Si/SiO_2 molar ratio = 2, $(Si + SiO_2)/C^*$ weight ratio = 2.5. The BET surfaces areas reported were those obtained after calcination of the SiC material after synthesis, in air at 600 °C for 2 h

	Reaction temperature (1250 °C)		Reaction temperature (1300 °C)	
Reaction duration (h)	BET surface area ($m^2 \cdot g^{-1}$)	$C^* \rightarrow$ SiC (%)	BET surface area ($m^2 \cdot g^{-1}$)	$C^* \rightarrow$ SiC (%)
1	112	16	65	32
2	77	26	—	—
3	60	39	31	63
4	49	46	—	—
5	46	59	26	77
7	41	62	14	79
10	26	70	10	85

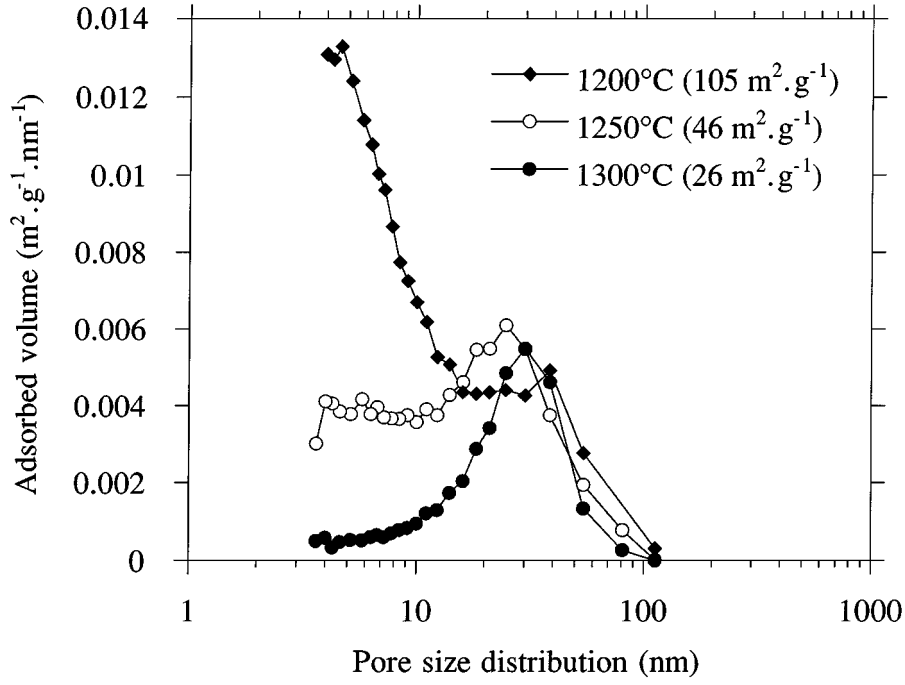

Figure 3 Pore size distribution of SiC materials synthesized at different reaction temperatures ranging from 1200 to 1300 °C. Reaction conditions: (Si/SiO_2) molar ratio = 2, $(Si + SiO_2)/C^*$ ratio = 2.5, reaction duration = 5 h.

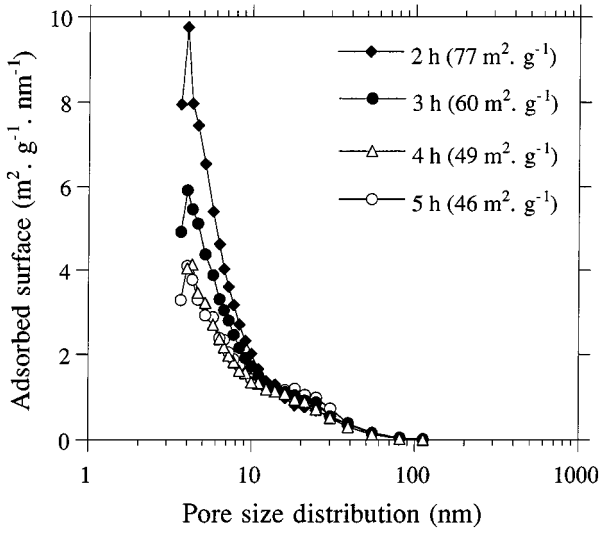

Figure 4 Pore size distribution of the SiC materials synthesized at 1250 °C as a function of the reaction duration. Reaction conditions: (Si/SiO_2) molar ratio = 2, $(Si + SiO_2)/C^*$ ratio = 2.5.

at the begining of the reaction (1 h) and then the surface slowly decreased as the duration of the synthesis and the conversion increased. The sample prepared at 1250 °C for 3 h exhibited a surface area after calcination of around 60 $m^2 \cdot g^{-1}$ and a $C^* \rightarrow SiC$ conversion of 36%. This surface area slowly decreased as a function of the reaction duration. However, it is significant to note that the carbon conversion was almost unchanged after 5 h of reaction. The influence of the reaction duration at 1250 °C on the pore size distribution of the calcinated SiC is presented in the Fig. 4. Increasing the reaction duration caused collapse of small size pores (4–5 nm) along with a decrease in the material surface area, as observed above. At relatively low temperatures the influence of reaction duration was negligible (Peschiera, 1993). It could thus be stated that a reaction temperature $\geq$1250 °C and a duration ~10 h allowed of a relatively high conversion (~80%), but accompanied by a drastic drop in the material surface area; i.e. at 1250 °C and 10 h of reaction the conversion was 70% whereas the surface area was only 26 $m^2 \cdot g^{-1}$ (Table II).

The results observed above show that high surface area SiC can be obtained by reacting the SiO vapor and activated charcoal at temperature around 1250 °C. However, reactions carried out at 1200 °C for 5 h have shown that, at such a low temperature, the SiC formation was strongly inhibited due to the low rate between the SiO vapor diffusion in and the carbon diffusion out whereas at temperatures $\geq$1250 °C the increase in the $C^* \rightarrow SiC$ conversion was obtained along with a drastic decrease in the material surface area due to the surface diffusion phenomenon which induced the disappearance of the small pores. The results of the synthesis at 1200 °C for 15 h with different $(Si + SiO_2)/C^*$ ratios are summarized in Table III. At high $(Si + SiO_2)/C^*$ weight ratio a high SiC yield can be obtained with a relatively high surface area. The surface area of the material remained unchanged at around 46–48 $m^2 \cdot g^{-1}$ when the $C^* \rightarrow SiC$ conversion was increased from 55 to 75%, which showed that the SiC surface area could be quite independent from the total conversion.

TABLE III Characteristics of SiC as a function of the $(Si + SiO_2)/C^*$ weight ratio. Reaction conditions: Si/SiO_2 molar ratio = 2, reaction temperature = 1200 °C, reaction duration = 15 h. The BET surfaces areas reported were those obtained after calcination of the SiC material after synthesis, in air at 600 °C for 2 h

$(Si + SiO_2)/C^*$ weight ratio	BET surface area ($m^2 \cdot g^{-1}$)	$C^* \rightarrow SiC$ conversion (%)
6	47	58
8	48	67
12	48	74

3.2. SiC characterization

The results obtained above have shown that the different synthesis parameters have a significant influence on SiC formation. However, these parameters only concern the total conversion and surface area of the final SiC whereas other physical characteristics, i.e. crystalline structure, resistance to oxidation and morphology of the material remain unchanged. The influence of these characteristics will be investigated below using a single material synthesized at 1250 °C for 7 h with a $(Si + SiO_2)/C^*$ ratio of 6.

3.2.1. XRD

The XRD patterns of the starting activated charcoal and of SiC, after synthesis and after calcination at 600 °C, are presented in Fig. 5. The XRD pattern of the activated charcoal (Fig. 5a) showed almost no diffraction lines and confirmed the amorphous character of the material. The XRD pattern of SiC after synthesis (Fig. 5b) showed the diffraction lines corresponding to the mixture of α- and β-SiC along with a broad peak at low diffraction angles, which corresponded to the presence of an amorphous phase in the sample. The amorphous phase could be the remaining activated charcoal inside the SiC matrix. No traces of other compounds such as Si or SiO_2 were detected meaning that such compounds were either present in very small crystalline amounts or in an amorphous form.

After calcination at 600 °C for 2 h in air, the broad peak at low diffraction angles had disappeared and only diffraction lines corresponding to silicon carbide were observed (Fig. 5c). The XRD pattern of the calcinated sample again showed no evidence of the formation of SiO_2 or other species meaning that during the calcination step no bulk oxidation of SiC occured. This meant that calcination at 600 °C allowed the complete removal of the remaining activated charcoal inside the SiC matrix.

3.2.2. Thermogravimetry analysis (TGA)

The TGA spectra of the activated charcoal and the SiC samples are presented in Fig. 6. The weight loss and differential analysis curves for the activated charcoal indicated that essentially all weight loss started at around 500 °C and corresponded to the total oxidation of the activated charcoal. On the SiC materials the weight loss started at a higher temperature, whatever the sample, meaning that the SiC coating acted as a diffusion barrier for the activated charcoal oxidation [19].

However, as can be seen on the TGA spectrum, a slow increase in weight was observed at a temperature of around 700 °C. This phenomenon was attributed to the oxidation of the silicon carbide itself ($SiC \rightarrow SiO_2$). It is well known that silicon carbide is not stable in air, in a thermodynamic sense, because it reacts with oxygen with a negative change in free energy. On the other hand, it is significant to note that the oxide film formed on the material surface may be protective and may force the oxidation rate to decrease with time. Finally, it should be pointed out that in many cases the material will be used in a reductive, or poorly oxidative atmosphere, in which the oxidation rate is not significant as already reported in the literature by several authors [20, 21].

3.2.3. Scanning electron microscopy (SEM)

SEM micrographs of the starting activated charcoal and the resulting SiC (after synthesis) are presented in Fig. 7. The low magnification SEM images, presented in Fig. 7a and c, show that the macroscopic shape of the activated charcoal was retained during the SiC synthesis.

A surface modification was observed at higher magnification and is presented in Fig. 7b and d. After synthesis an important morphology change was observed: the smooth surface of the activated charcoal (Fig. 7b) was completely transformed into an aggregate structure (Fig. 7d). The morphology observed on the SiC samples after synthesis was retained after calcination at 600 °C for 2 h, meaning that the material was stable after this treatment.

3.2.4. High-resolution transmission electron microscopy (HRTEM)

The TEM micrograph of the SiC material obtained is presented in Fig. 8 and shows the presence of aggregated particles of SiC, almost no amorphous phase is observed. After calcination at 600 °C in air, all the remaining activated charcoal had disappeared. High resolution TEM micrographs showed that the silicon carbide prepared by the gas-solid reaction contained a significant density of stacking faults and microtwins along the [111] direction. The presence of the stacking faults can be viewed in Fig. 8 (low magnification): the stacking faults are revealed on the TEM micrographs as black stripes in the grains. A relatively large faulted region can be observed from a few tens of nanometers up to a few micrometers in size. High-resolution TEM micrograph (Fig. 9) shows the atomic scale view of the SiC surface and stacking faults along the [111] direction. A similar result has been reported by Pezzotti *et al.* [22] during their investigation of the microstructure of the SiC platelet by HRTEM.

In contrast to the XRD data, which gave an average picture of a large portion of the sample, TEM analysis allowed the observation of a very small zone (microstructure analysis). The HRTEM micrograph (Fig. 9) shows that the material obtained was covered by an amorphous phase (thickness ca. 2–3 nm) which was not detected by XRD. The existence of such a phase has been reported by different authors in the literature [23–25] and has been attributed to SiO_2 or SiO_xC_y phase. The precise composition of such a phase was not straightforward due to the amorphous character of the sample. Previous HRTEM analysis coupled with Energy Dispersive X-Ray Spectroscopy (EDS) have shown that this amorphous phase was composed of Si, C and O. However, precise quantification was not possible.

4. Discussion

4.1. Structural changes

It was clear that high surface area silicon carbide could easily be obtained from the gas-solid reaction between

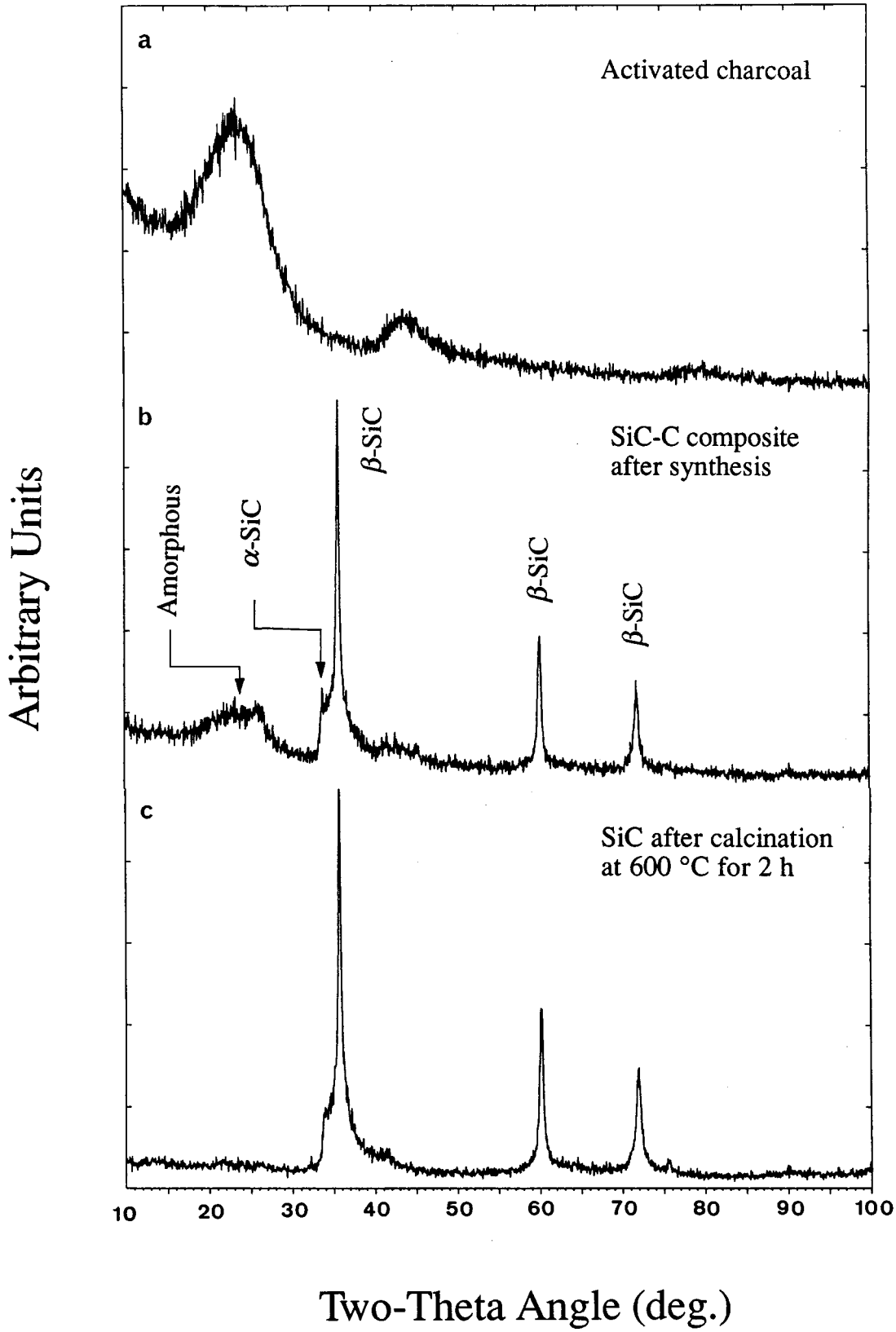

Figure 5 XRD patterns of the active carbon, SiC after synthesis and after calcination in air at 600 °C for 1 h. The diagrams were recorded with a step of 0.05 degree (2θ) and a scan time of 10 s. In an inset a portion of the SiC XRD pattern was recorded with a step of 0.02 degree (2θ) and a scan time of 20 s.

SiO and C. Different shaped SiC obtained by preshaping the starting activated charcoal: grain, extrudate or monolith could thus be formed. The silicon carbide formed retained the macroscopic structure of the starting activated charcoal, as shown in Fig. 7. The results observed meant that the transformation of the activated charcoal into SiC proceeded via a topotactic transformation where one carbon was replaced by one Si with a concomitant formation of one CO molecule. Such a transformation should also lead to the formation of pores inside the carbon grains which were the precursor of the final porosity of the SiC material. This allowed

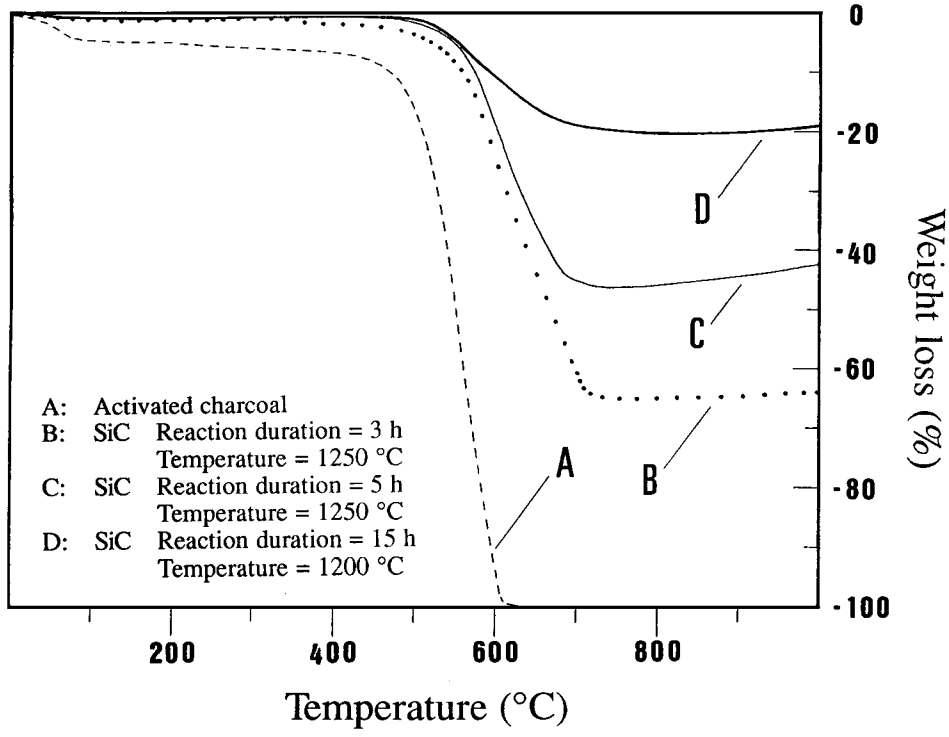

Figure 6 Thermogravimetry analysis of the active carbon and SiC materials after synthesis under different reaction conditions.

the obtention of a high surface area SiC. However, due to the fact that the material was the result of the reaction between SiO gas and C solid, along this reaction, layers of SiC were formed on the microscopic surface (and not a crust on the macroscopic surface) which rendered transformation of the carbon bulk more and more difficult, limited by the diffusion of SiO through these layers of SiC, as previously reported by Ledoux and co-workers [26] during the synthesis of transition metal carbides (Mo_2C, WC and VC_{1-x}) using a similar gas-solid reaction.

The SiC material in this work was not structurally pure but was composed of a mixture of two polymorphs of SiC: α (hexagonal structure, 2H, 4H, 6H, ...) and β (cubic structure, 3C) as observed by XRD data and HRTEM. This phenomenon was attributed to the presence of a high density of stacking faults in the [111] direction of the material as already observed by Benaissa *et al.* [14, 27], Koumoto *et al.* [28] and by HRTEM results obtained in this work.

HRTEM micrograph (Fig. 9) also showed the presence of an amorphous layer (thickness ca. 2–3 nm) on the material surface. The nature (SiO_2 or SiO_xC_y) of this phase is still a matter of controversy in the literature. Recently, it has been reported by Benaissa *et al.* [14], using HRTEM, that the surface of SiC was covered with an amorphous layer which could be attributed to SiO_2 or oxycarbide species with a thickness of 1–3 nm. Similar results had already been reported in the literature by several authors using surface techniques (XPS, AES) [19, 29]. The product formed was similar, whatever the reaction conditions used, i.e. reaction temperature and duration and the $(Si + SiO_2)/C^*$ ratio, which means that under the reaction conditions described above, silicon carbide is the principal product. Porte and Sartre [23] and Bouillon *et al.* [24] had reported the existence of a silicon oxycarbide phase which exhibited a Si XPS binding energy different to the one found on SiO_2 (101.5 eV instead of 103.1 eV for SiO_2). Similar results were also reported by Mozdzierz *et al.* [25] using a combination of different characterization techniques (EELS, HRTEM and EDX). The chemical composition of the amorphous phase determined from these techniques was $SiO_{1.52}C_{0.6-1.05}$. The existence of SiO_2 and not an oxycarbide on the surface of SiC was reported by Moene [21] using the DRIFT technique; the absorption spectrum showed the presence of three absorption bands located at 790, 900 and around 1100 cm^{-1} which could be attributed to the Si-C vibrations (790 and 900 cm^{-1}) and the asymmetric stretching vibration of the Si-O groups. However, TPR analysis performed by Moene and co-workers [21] on the Ni, Cu, Co and Mo oxides supported on as-prepared SiC displayed a lower reduction temperature compared to that obtained with the same oxides prepared and treated under similar conditions but supported on bulk SiO_2. This led to the conclusion that the oxidic layer on the SiC surface was not similar to SiO_2. The most probable interpretation about the nature of the amorphous phase on the SiC surface is to assume the existence of a mixture of SiO_2 and SiO_xC_y phases as already observed by XPS techniques (not shown).

During the course of the transformation of the activated charcoal to SiC, an important surface area loss was observed whatever the reaction conditions. This surface area loss could be attributed to the transformation of the micropores of the starting activated charcoal into meso- and macropores resulting in a lower surface area. The loss could also be attributed to a structural rearrangement of the activated charcoal itself. It was observed by Benaissa *et al.* [30] that during the course of the reaction, the amorphous active carbon, constituted of aggregated basic structural units (BSUs) [31], underwent structural rearrangement diminishing

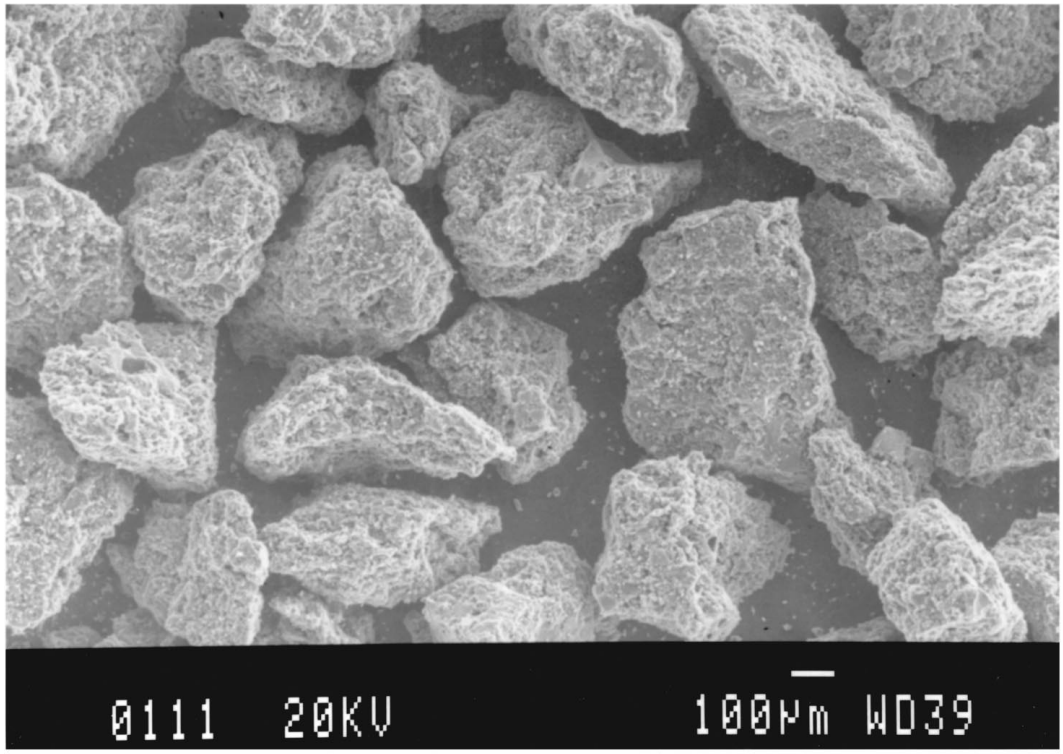

(a)

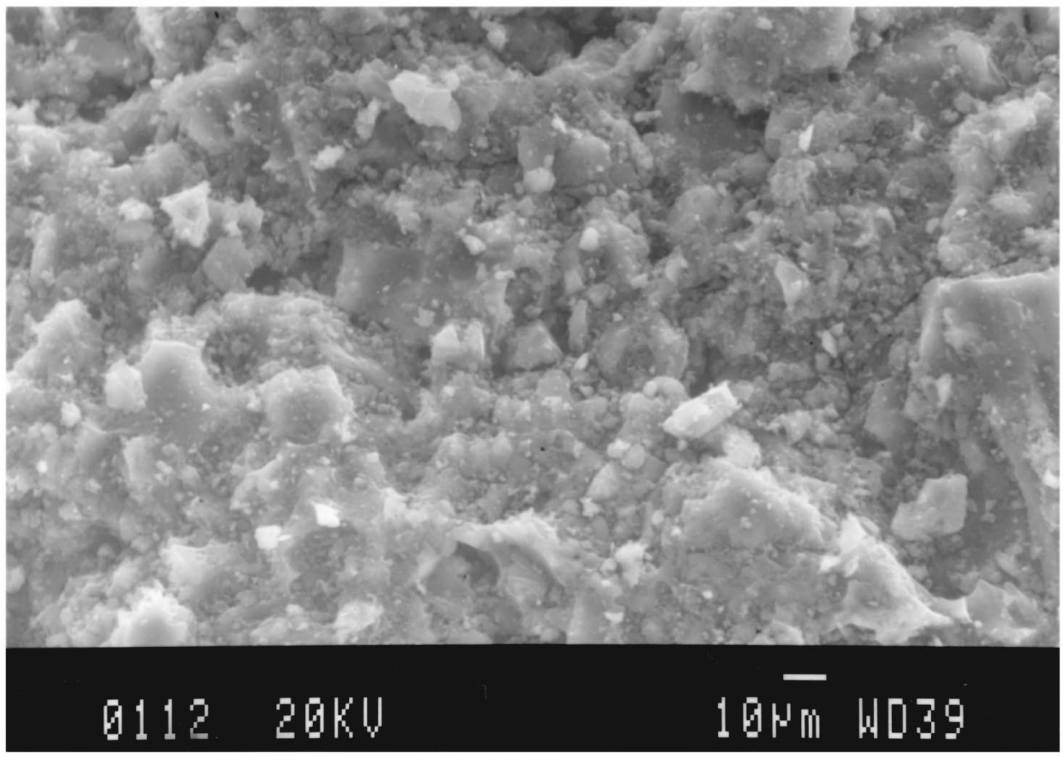

(b)

Figure 7 SEM micrographs of the active carbon (7a, b) and SiC (7c, d) after synthesis. The white bar represents 100 μm for Figs a and c and 10 μm for Figs b and d. (*Continued*).

the number of initial sites accessible by SiO. Therefore, the proportion of reactive sites of the highly reactive prismatic plane exposed at the active carbon surface was greater in the first stages of the reaction and rapidly chemisorbed SiO molecules. This provided random nucleation sites for silicon carbide in the active carbon matrix [Benaissa *et al.*] during and immediately after the start of the reaction because the BSUs were randomly distributed. As the reaction proceeded, ordering processes occured within BSUs by removing functional goups, reducing the number of surface reactive sites. This growth mode affected the conversion rate since the re-organized active carbon did not react with SiO. The reconstruction of the activated charcoal also explained the increase in oxidation temperature of the remaining charcoal in the core of the final sample where

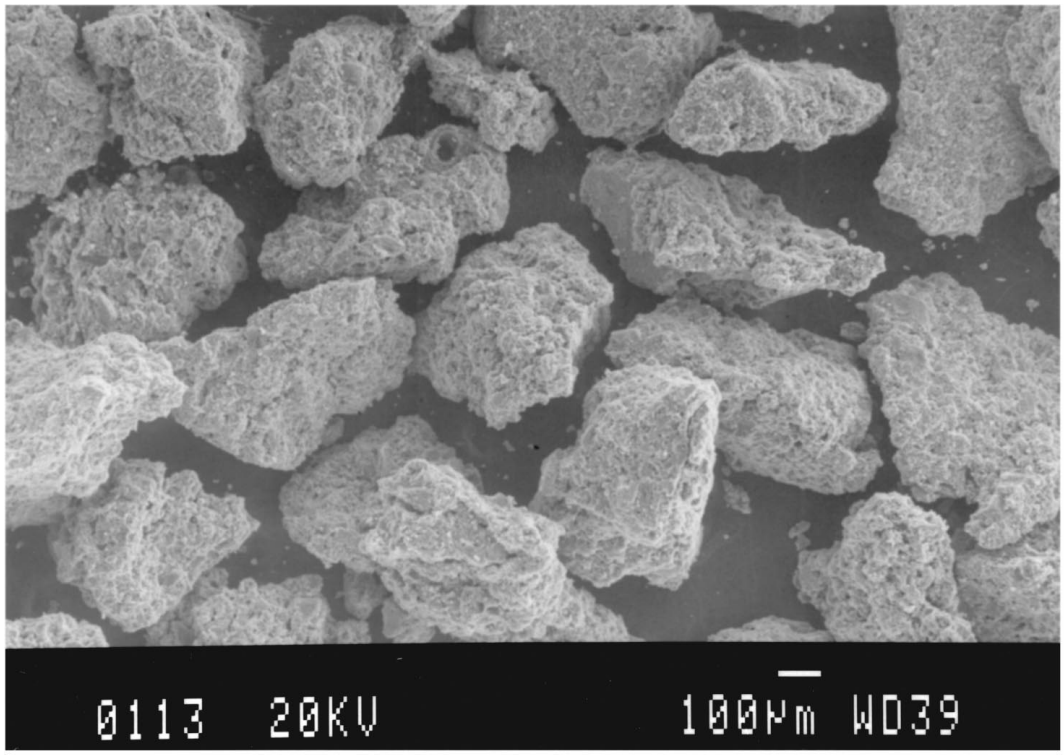

(c)

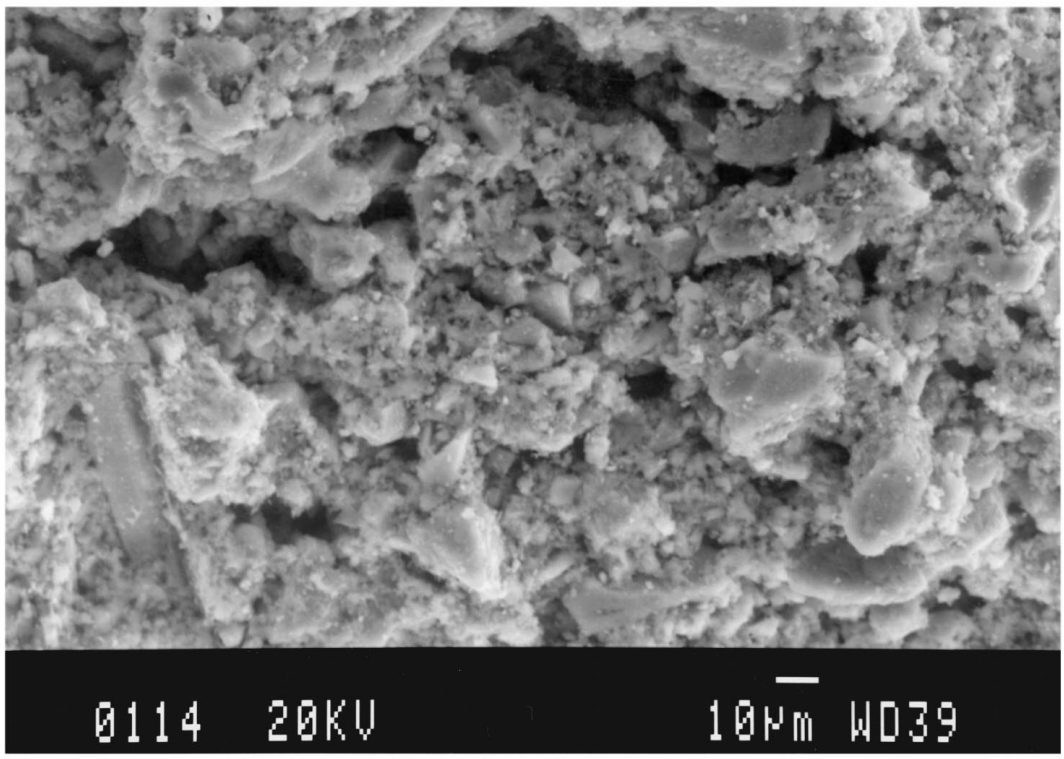

(d)

Figure 7 (*Continued*).

compared to the oxidation temperature of the initial charcoal.

A subsequent calcination of the SiC (after synthesis) at 600 °C for 2 h induced a further loss in surface area by burning the remaining activated charcoal located in the core of the material. However, the second loss in surface area was less significant compared to the theoretical surface area loss corresponding to the remaining activated charcoal determined before and after calcination at 600 °C. This could be explained by the fact that in the sample before calcination, a fraction of the high surface area activated charcoal located in the bulk of the material was not accessible to the adsorbant gas (N_2) and so was not totally taken into account in the measured surface area. This fact was also supported by the TGA results where the starting temperature of the weight loss of the sample increased as the conversion of the activated charcoal into SiC increased. The final material

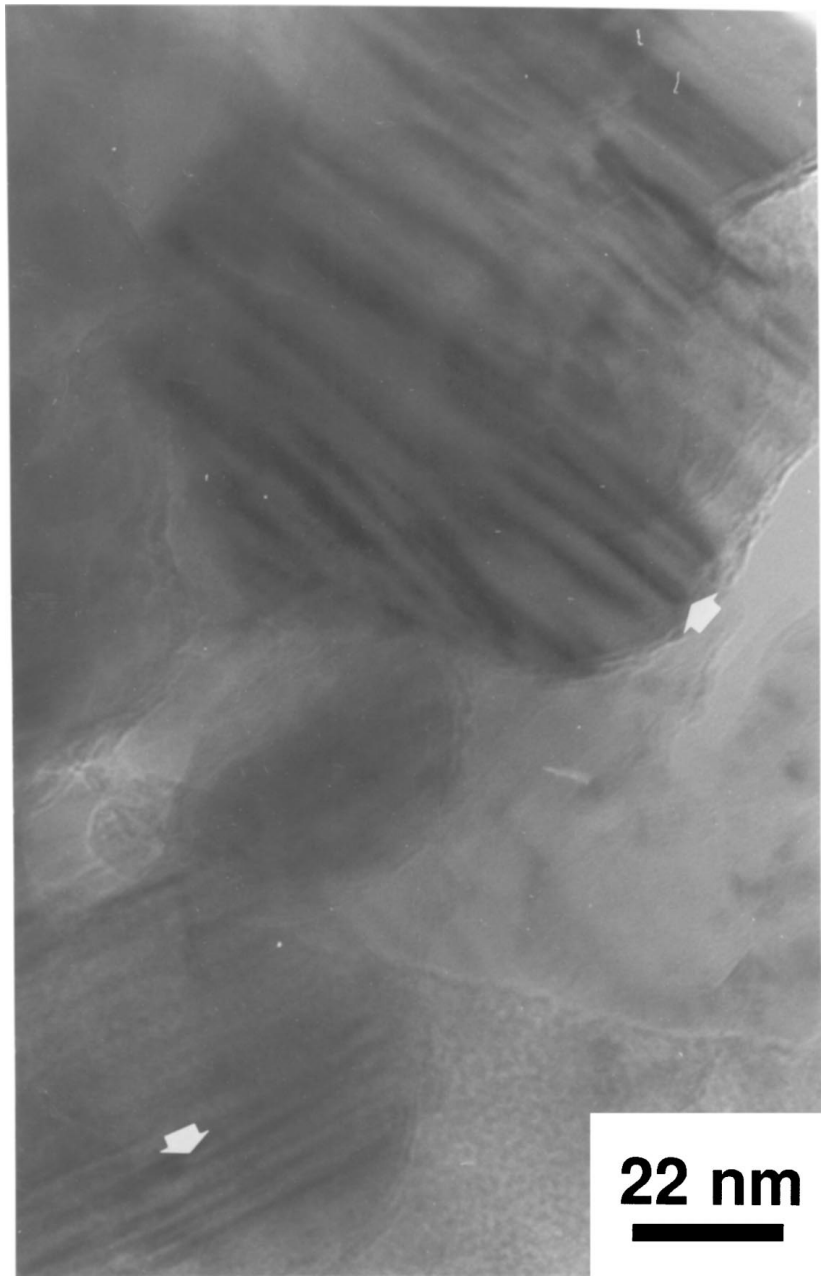

Figure 8 TEM micrograph of the SiC after synthesis. The stacking faults visualized as black strips were indicated by arrows.

exhibited a higher thermal resistance compared to the starting activated charcoal as evidenced by the TGA spectra presented in Fig. 6. Similar results had already been reported by Stegenga [29] during an attempt to cover the activated charcoal by layers of SiC in order to increase the material resistance to oxidation for high temperature reaction experiments. In this case, the SiC layers played a protective role which rendered oxygen diffusion toward the bulk material more difficult.

4.2. Influence of the synthesis parameters

4.2.1. Si to SiO_2 ratio

The total conversion of the final material was significantly influenced by the molar ratio of the Si and SiO_2 mixture: the higher the Si to SiO_2 molar ratio, the higher the total conversion. It appeared that silicium present in excess could led to the formation of a larger amount of SiO vapour which would increase the rate of the reaction by simple kinetic effects. This hypothesis could be explained by the mechanism of the SiO vapour generation. Under the reaction conditions, several mechanisms could be proposed for the generation of SiO vapour, according to Equation 1: (i) the two step mechanism passing through a gaseous intermediate and (ii) the solid-solid reaction.

A two step mechanism has been reported by Kennedy and North [32] in their study, in which Si vapour reacts with SiO_2 to generate SiO vapour according to the following equations

$$Si_{(s)} \rightarrow Si_{(g)}$$

$$Si_{(g)} + SiO_{2(s)} \rightarrow 2SiO_{(g)}$$

Studies ruled out this mechanism as the principal mechanism in the work reported in the present article. In Fig. 10 is reported the evolution of the weight loss of the Si/SiO_2 mixture as a function of the reaction duration at different temperatures which allowed the calculation of the apparent activation energy needed for

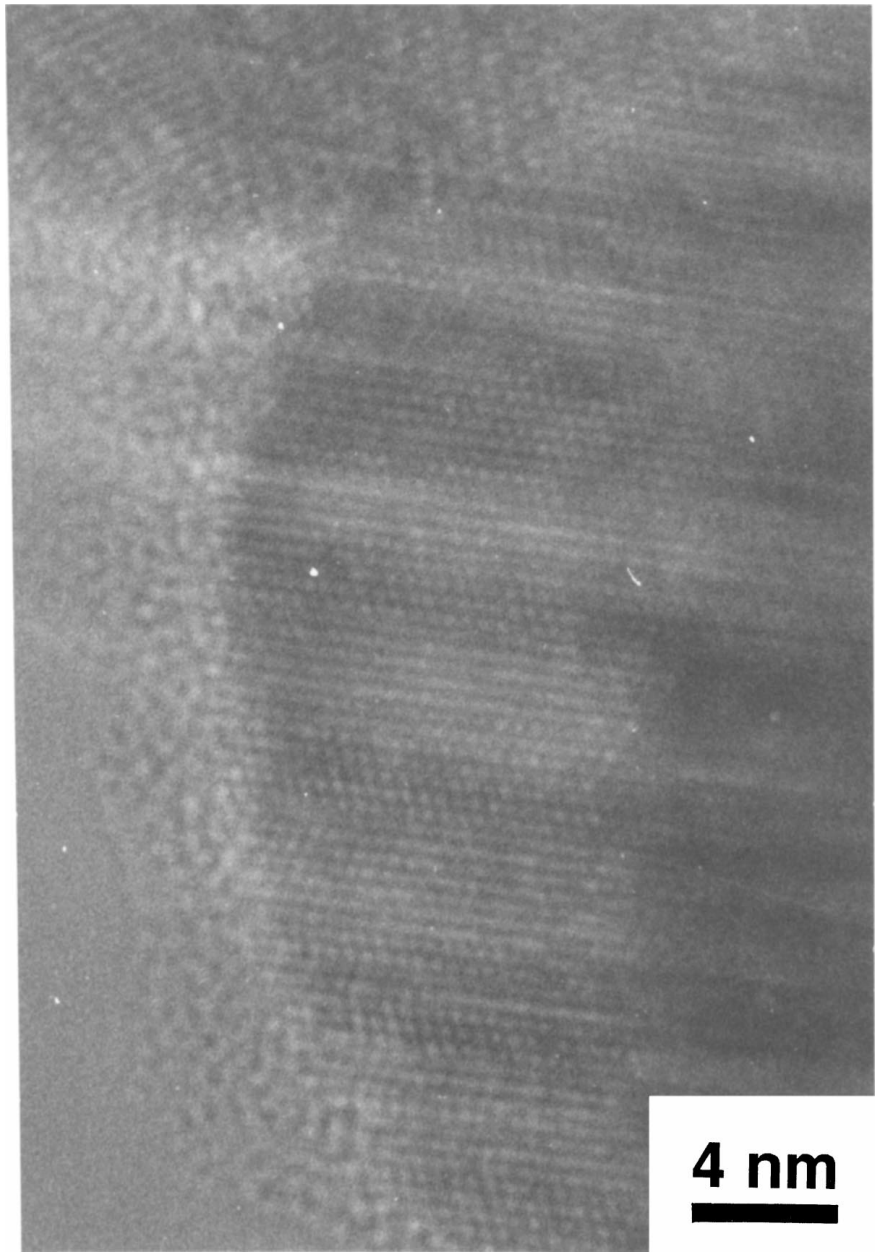

Figure 9 HRTEM micrograph of the SiC material showing the presence of a high density of stacking faults along the [111] axis and an amorphous layer on the surface.

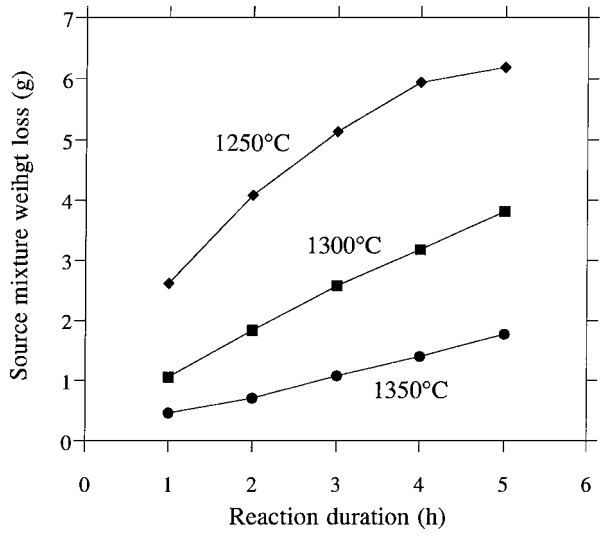

Figure 10 Influence of reaction duration on the source mixture weight loss at different temperatures. Reaction conditions: (Si/SiO_2) molar ratio = 2, (Si + SiO2)/C* ratio = 2.5.

the generation of SiO vapour: 250 $kJ \cdot mol^{-1}$ whereas for the two successive steps mechanism the activation energy for Si sublimation was 451 $kJ \cdot mol^{-1}$ [33]. If the two step mechanism was effective, a change in the surface area of SiO_2 should have an effect on the SiO generation, which was not the case [18].

On the other hand, a solid-solid reaction thesis was in agreement with all experimental studies. A study by Peschiera [18] on the SiC synthesis, had shown the influence of the Si granulometry and of the initial mixture densification on the contact surface of the source mixture. The last phenomenon, well known for solid-solid powder reactions, was reported by Beretka [34] and Sasaki [35].

Such a result explained well that the SiO concentration was directly linked to the Si/SiO_2 molar ratio: as the SiO vapor was generated via a solid-solid reaction between Si and SiO_2, increasing the Si concentration probably led to an increase in the surface contact between the Si and SiO_2 compounds.

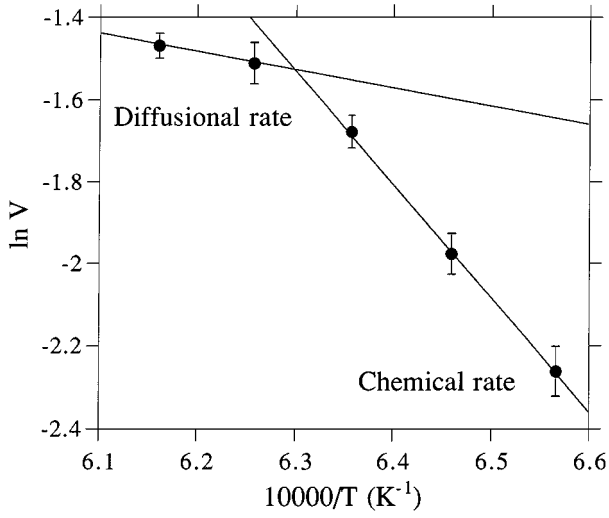

Figure 11 Evolution of the average rate of carbide formation (V) as a function of the reaction temperature.

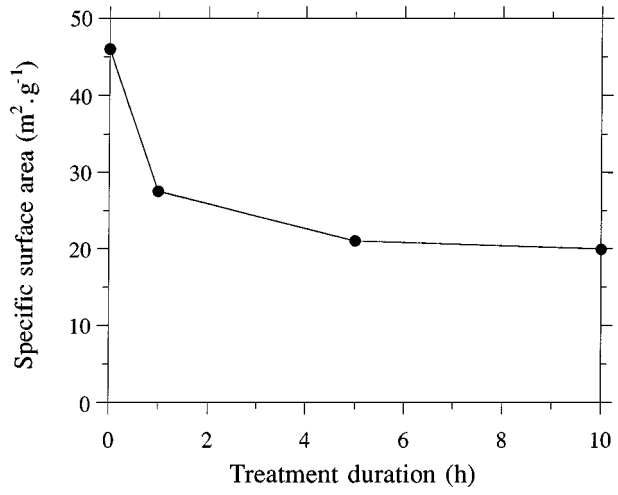

Figure 12 Influence of a post-synthesis thermal treatment on the specific surface area of SiC material.

However, a high Si/SiO_2 molar ratio (>2) led to a reverse trend and resulted in a SiC yield drop. This phenomenon was attributed to the excessive generation of the SiO vapour during the first hours of heating which could have escaped leading to a SiO deficiency for the rest of the synthesis and thus, decreasing the total conversion.

4.2.2. Temperature and duration on the SiC formation

The results have shown that the reaction temperature had a significant effect on the final surface area of the material: at 1200 °C the surface area was $105\,m^2 \cdot g^{-1}$, whereas at 1300 °C the surface area was only 26 $m^2 \cdot g^{-1}$. A first hypothesis could be proposed to explain this result: at high reaction temperature (1300 °C) the SiC initial nucleï rapidly sintered resulting in large SiC particles with low surface area. A second way to explain this result was to consider surface diffusion phenomena.

Fig. 11 presents the Arrhenius plot of the evolution of the logarithm of the rate of formation of the carbide obtained by averaging many reactions (weight increase per hour with a reaction duration of 7 h) as a function of the reverse reaction temperature. The SiC rate of formation exhibited two different regimes according to the reaction temperatures used. At low reaction temperature, the SiC formation rate was apparently limited by the SiO generation (chemical rate limitation), whereas, at higher reaction temperatures, the SiC formation rate was significantly increased. At such a high rate the diffusion of CO out of the bulk and of SiO into the matrix could become the limiting effect, the other kinetic factors being negligeable. A similar double regime was already described and known as the "Shrinking Core Model" by Hurst *et al.* [36] and by Falconer and Schwartz [37] for oxide material reduction. At the beginning of the reaction, the reactive surface was at its highest area and then, continuously shrunk as SiC progressively covered the carbon, increasing the difficulty for SiO and CO to diffuse. This transition was also related by Scott Fogler [38]. The activation energy, in the domain of chemical kinetics, was calculated at 233 $kJ \cdot mol^{-1}$, confirming that the SiO vapor generation was the limiting step.

The SiC yield was significantly improved up to 70–85% by increasing the reaction duration at 1250 °C or at 1300 °C (Table II). The relatively low surface area obtained (20–26 $m^2 \cdot g^{-1}$) when increasing the duration of the reaction was attributed to a surface diffusion phenomenon reorganizing the surface at a lower energy level by filling the pores. This phenomenon was well illustrated by the porosimetry reported in Figs 3 and 4. Similar observations were reported by Elder and Krstic [39] and Hase *et al.* [40] who observed that SiC started to sinter, by surface diffusion, at a temperature lower than the theoretical sintering temperature. This sintering process was proportional to the surface energy of the material. The surface energy increases as the specific surface area of the material is increased.

In order to prove this surface rearrangement the following experiment was carried out a batch of SiC synthesized at 1250 °C for 5 h with a surface area of 46 $m^2 \cdot g^{-1}$ (after calcination) was treated again under dynamic vacuum at the same temperature well below the theoretical temperature of sintering (2000 °C), for different durations without reactants, neither carbon nor SiO. The evolution of the surface area of the sample is presented in Fig. 12. After 1 h the surface area dropped to 26 $m^2 \cdot g^{-1}$ and then slowly diminished to reach 20 $m^2 \cdot g^{-1}$ after 10 h. This rapid collapse due to the disappearance of the smallest pores (higher surface energy) confirmed the proposed mechanism. At 20 $m^2 \cdot g^{-1}$ the surface seemed to have reached a low stable energy state.

4.2.3. Influence of the $(Si + SiO_2)/C^*$

From all the preceding results it could be concluded that a high surface area SiC could be obtained at 1250 °C within a short reaction time. A higher temperature and a too long reaction duration would have a negative effect both on the structure of the carbon (reconstruction which decreases the number of reactive sites) and on the final porosity of SiC (diffusion and sintering). However, a low reaction temperature and a short reaction

duration would give a too low total conversion. Low conversion leads to a weaker strength of the SiC grain after burning the unreacted charcoal inside the material. The remaining solution was to increase the relative partial pressure of SiO which was shown as a very positive factor in the kinetics of the reaction. When the ratio $(Si + SiO_2)/C^*$ was increased, which was the way to increase the relative partial pressure of SiO, the conversion of the activated charcoal was greatly increased. Even at 1200 °C, a very low temperature, stable surface areas ($>46\,m^2 \cdot g^{-1}$) after calcination could be obtained at relatively high conversion (>75%).

5. Conclusion

High surface area SiC ($\geq 48\ m^2 \cdot g^{-1}$) was prepared from the gas-solid reaction between SiO vapor and activated charcoal according to the method developed by Ledoux and co-workers. The size and shape of the final ceramic was controlled by pre-shaping the starting charcoal as the macroscopic shape of the charcoal was retained after the reaction. The reaction temperature had a significant influence on the final surface area of the material: at reaction temperatures higher than 1300 °C, a drastic loss in surface area was observed due to the collapse of particles resulting in the disappearance of small pores between 5 and 10 nm. Secondarly, the reaction duration had a significant influence on the final surface area of the material, especially when the reaction was conducted at temperatures higher than 1250 °C. The synthesis conducted at relatively low temperature (1200 °C) and long reaction duration (15 h) with a high ratio (Si and SiO_2)/ activated charcoal allowed the formation of a SiC with a medium surface area ($40–50\ m^2 \cdot g^{-1}$) and a high C to SiC yield. To improve this surface area, the use of dopants have proved to be a very efficient method and these results will be published later.

Acknowledgements

This work is supported by a contract with the Pechiney Company. SEM observations and TGA experiments were performed at the Groupe des Matériaux Inorganiques of the Institute of Chemistry and Physic of Materials of Strasbourg (ECPM-ULP-CNRS). Dr. E. Peschiera is also gratefully acknowledged for performing a part of the synthesis experiments.

References

1. M. F. M. ZWINKELS, S. G. JARAS, P. G. MENON and T. A. GRIFFIN, *Catal. Rev. Sci. Eng.* **35** (1993) 319.
2. P. BURTIN, J. P. BRUNELLE, M. PIJOLAT and M. SOUSTELLE, *Appl. Catal.* **34** (1987) 239.
3. J. A. SCHWARTZ, C. CONTESCU and A. CONTESCU, *Chem. Rev.* **95** (3) (1995) 475.
4. H. C. YAO, H. K. STEPIEN and H. S. GANDHI, *J. Catal.* **61** (1980) 547.
5. H. J. SANDERS, *Chem. Eng. News* **62** (1984) 26.
6. M. J. LEDOUX, S. HANTZER, J. GUILLE and D. DUBOTS, US Patent no. 4.914.070.
7. M. J. LEDOUX, S. HANTZER, C. PHAM-HUU, J. GUILLE and M. P. DESANEAUX, *J. Catal.* **114** (1988) 176.
8. M. J. LEDOUX, J. GUILLE, S. HANTZER, S. MARIN and C. PHAM-HUU, "EA of the MRS," edited by E. W. Corcoran Jr. and M. J. Ledoux, 1990, p. 135.
9. M. J. LEDOUX and C. PHAM-HUU, *Catal. Today* **15** (1992) 263.
10. D. A. WHITE, S. M. OLEFF and J. R. FOX, *Adv. Ceram. Mater.* **2** (1987) 53.
11. K. B. TRIPLETT, J. H. BURK, F. G. SHERIF and W. VREUGDENHIL, US Patent no. 5.338.716 (1994).
12. R. W. CHORLEY and P. W. LEDNOR, *Adv. Mater.* **3** (1991) 474.
13. W. M. CARTY and P. W. LEDNOR, *Current Opinion Solid State Mater. Sci.* **1** (1996) 88.
14. M. BENAISSA, C. PHAM-HUU, C. CROUZET, J. WERCKMANN and M. J. LEDOUX, *Catal. Today* **23** (1995) 263.
15. C. PHAM-HUU, P. DEL GALLO, E. PESCHIERA and M. J. LEDOUX, *Appl. Catal. A: General* **132** (1995) 77.
16. A. PHILIPPE, J. NOUGAYREDE, S. SAVIN-PONCET, M. J. LEDOUX, C. PHAM-HUU and C. CROUZET, French Pat. Appl. no. 94-13752 (1994).
17. J. H. DE BOER, in "The Structure and Properties of Porous Materials," edited by D. H. Everett, 1958.
18. E. PESCHIERA, PhD Dissertation, University of Strasbourg, 1993.
19. H. VINCENT, J. L. PONTHENIER, L. PORTE, C. VINCENT and J. BOUIX, *J. Less Comm. Met.* **157** (1990) 1.
20. P. W. LEDNOR, *Catalysis Today* **15** (1992) 243.
21. R. MOENE, PhD Dissertation, University of Delft, 1995.
22. G. PEZZOTTI, B. T. LEE, K. HIRAGA and T. NISHIDA, *J. Mater. Sci.* **28** (1993) 4787.
23. L. PORTE and A. SARTRE, *ibid.* **24** (1989) 271.
24. E. BOUILLON, D. MOCAER, J. F. VILLENEUVE, R. PAILLER, R. NASLAIN, M. MONTHIOUX, A. OBERLIN, C. GUIMON and G. PFISTER, *ibid.* **26** (1991) 1517.
25. N. MOZDZIERZ, M. BACKHAUS-RICOULT and D. IMHOFF, in Proceedings of the 13th International Congress on Electron Microscopy, 1994, p. 325.
26. M. J. LEDOUX, J. GUILLE, C. PHAM-HUU and S. MARIN, US Patent no. 5.391.524.
27. M. BENAISSA, J. WERCKMANN, J. L. HUTCHISON, E. PESCHIERA, J. GUILLE and M. J. LEDOUX, *J. Crystal Growth* **131** (1993) 5.
28. K. KOUMOTO, S. TAKEDA, C. H. PAI, T. SATO and H. YANAGIDA, *J. Amer. Ceram. Soc.* **72** (10) (1989) 1985.
29. S. STEGENGA, M. VAN WAVEREN, F. KAPTEIJN and J. A. MOULIJN, *Carbon* **30** (1992) 577.
30. M. BENAISSA, J. WERCKMANN, G. EHRET, E. PESCHIERA, J. GUILLE and M. J. LEDOUX, *J. Mater. Sci.* **29** (1994) 4700.
31. A. OBERLIN, *Carbon* **22** (1984) 521.
32. P. KENNEDY and B. NORTH, *Proc. Br. Ceram. Soc. Sci.* **33**(3) (1983) 1.
33. Janaf Thermochemical Tables, United States National Bureau of Standards, 2nd ed., 1971.
34. J. BERETKA, *J. Amer. Ceram. Soc.* **67**(9) (1984) 615.
35. H. SASAKI, *ibid.* **50**(7) (1967) 378.
36. N. W. HURST, S. J. GENTRY, A. JONES and B. D. MCNICOL, *Catal. Rev.-Sci. Eng.* **24** (1982) 233.
37. J. L. FALCONER and K. A. SCHWARTZ, *ibid.* **25** (1983) 141.
38. H. SCOTT FOGLER, "Elements of Chemical Reaction Engineering" (Prentice-Hall Edition, 1992) p. 620.
39. P. ELDER and V. D. KRSTIC, *J. Mater. Sci. Lett.* **8** (1989) 941.
40. T. HASE, B. W. LIN, T. ISEKI and H. SUZUKI, *ibid.* **5** (1986) 69.

Received 6 February
and accepted 30 November 1998